

# Growth of the Turbulent Wake behind a Supersonic Sphere

CHARLES H. MURPHY<sup>1</sup> AND ELIZABETH R. DICKINSON<sup>2</sup>

*Ballistic Research Laboratories, Aberdeen Proving Ground, Md.*

Experimental data are presented on the growth of turbulent wakes up to 8000 calibers behind  $\frac{1}{4}$ -in. and  $\frac{1}{8}$ -in. spheres traveling at supersonic velocities. Experimental determination of the exponential coefficient in the growth law is very difficult, if not impossible. Data are presented in the form of both  $r = f(x^{1/3})$  and  $r = f(x^{1/2})$ . In the  $x^{1/2}$  representation, two regions of different wake growths are observed. By means of a quasi-steady state assumption, the effect of drag deceleration is eliminated and growth of the far wake compared with theoretical predictions. The agreement with the Lees-Hromas theory in this region was found to be quite good.

## Nomenclature

$C_D$	= drag coefficient
$d$	= diameter
$E$	= entrainment constant
$K$	= constant of the Lees-Hromas theory
$m$	= mass of sphere
$r$	= radius of turbulent wake in calibers (where a caliber is the diameter of the sphere)
$x$	= distance from center of sphere in calibers
$u$	= velocity of sphere
$\rho$	= air density

At the present time, there is a great deal of interest in the growth of turbulent wakes behind bodies traveling at hypersonic and high supersonic velocities. Theoretical studies usually confine themselves to dimensional reasoning to obtain a  $\frac{1}{3}$ -power growth law (1),<sup>3</sup> although Morton (2) and Lees and Hromas (3) have made use of physical assumptions on the mixing processes and derived more detailed results. Relatively little has been published on the results of experimental work, and what has been published is not in very good agreement. Cooper and Lutzky (4) have concluded that the wake radius in calibers,  $r$ , varies as the cube root of the distance  $x$  measured in calibers behind the body. Billerbeck (5) also concluded, though admittedly on the basis of a very limited amount of data, that  $r$  varies as  $x^{1/3}$ . On the other hand, Dana and Short (6), on the basis of measurements up to 300 calibers behind the body, concluded that the wake diameter in calibers,  $d$ , varies as  $x^{2/3}$  as far as  $x = 100$  and then as  $x^{1/3}$  up to  $x = 300$ . Slattery and Clay (7), however, on the basis of measurements up to 3500 calibers, concluded that, at atmospheric pressures,  $d$  varies as  $x^{1/2}$ , and at pressures of 41 and 100 mm Hg,  $d$  varies as  $x^{1/2}$  for about the first 50 calibers and thereafter as  $x^{1/3}$ .

Because of these varying conclusions drawn from experimental work and the uncertainties of the theoretical predictions, it became of interest to attempt to obtain more experimental data on wake growth.

## Experiment

Both  $\frac{1}{4}$  and  $\frac{1}{8}$ -in. steel spheres were fired through the Free-Flight Aerodynamics Range (8) of the Ballistic Research Laboratories. Instead of the standard setup for taking successive spark photographs as the sphere traveled downrange, a special setup was made for this program. The first arrangement of 16 plates for taking spark photographs of the wake is shown in the schematic diagram at the top of Fig. 1. All of the stations indicated were so wired that the sparks flashed

Received by ARS June 5, 1962; revision received September 23, 1962.

<sup>1</sup> Chief, Free Flight Aerodynamic Branch. Member AIAA.

<sup>2</sup> Aeronautical Research Engineer.

<sup>3</sup> Numbers in parentheses indicate References at end of paper.

simultaneously when the sphere was opposite the last plate at station 8.

Unfortunately, a piece of the sabot followed after the  $\frac{1}{4}$ -in. sphere fired through this setup, so that plates from stations 3 through 8 only were usable. The  $\frac{1}{8}$ -in. sphere was fired successfully. Thus, wake measurements were made for about 1200 calibers behind the  $\frac{1}{4}$ -in. sphere and for about 4400 calibers behind the  $\frac{1}{8}$ -in. sphere. The muzzle velocity of the  $\frac{1}{4}$ -in. sphere was 6400 fps; that of the  $\frac{1}{8}$ -in. was 7100 fps. The velocities of the spheres at the time the spark photographs were taken were 5300 and 3600 fps, respectively.

In order to obtain photographs of a greater length of wake, the range setup was then changed to the 20-plate arrangement shown at the bottom of Fig. 1. Again, a  $\frac{1}{4}$ -in. sphere and a  $\frac{1}{8}$ -in. sphere were fired. Complete sets of wake photographs were obtained from these firings. The muzzle velocity of the  $\frac{1}{4}$ -in. sphere was 7600 fps; that of the  $\frac{1}{8}$ -in. was 8100 fps. The velocities of the spheres at the time the spark photographs were taken were 4400 and 2650 fps, respectively. Wake measurements were made for about 4400 calibers behind the  $\frac{1}{4}$ -in. sphere and for about 8700 calibers behind the  $\frac{1}{8}$ -in. sphere.

The wake photographs were taken on  $11 \times 14$  in. glass plates. Because the diameter of a turbulent wake varies greatly in a short distance due to the growth and shrinkage of "bubbles," it was decided to measure the diameter at  $\frac{1}{2}$ -in. intervals along the 11-in. width of each plate. It must be pointed out, however, that the wake is free from other disturbances for only the first few feet behind the sphere. Thereafter, the shock wave of the sphere is reflected from the spark photography stations and passes through the wake. The effect on wake growth of the passage of this reflected shock wave through the wake is not known.

The accuracy of the diameter measurements is approximately 0.02 in. and that of the distance, approximately 0.1 in.

## Results

The first question that arose was how to use the large number of measurements (there were about 1400 measured points). It was decided arbitrarily that a beginning would be made by averaging the wake diameter for each plate. Thus, a reasonable number of data points became available for study.

In some of the references cited, there is a log-log plot of  $r$  or  $d$  vs  $x$ . It should be noted that, in an equation of the type  $r = r_0 + bx^\alpha$ , the slope of the log-log plot of  $r$  vs  $x$  equals  $\alpha$  only when  $r_0$  equals 0.

Hence, for values of  $x$  greater than 200, a least-squares solution was made of the equation  $r = r_0 + bx^\alpha$ , setting  $\alpha$  equal to  $\frac{1}{2}$  and to  $\frac{1}{3}$  for both the  $\frac{1}{4}$ -in. and the  $\frac{1}{8}$ -in. spheres. Because the difference between the solutions for the two sizes was about the same as the experimental error, a common solution was then made for both sizes. For  $\alpha = \frac{1}{2}$ ,  $r_0$  was small:

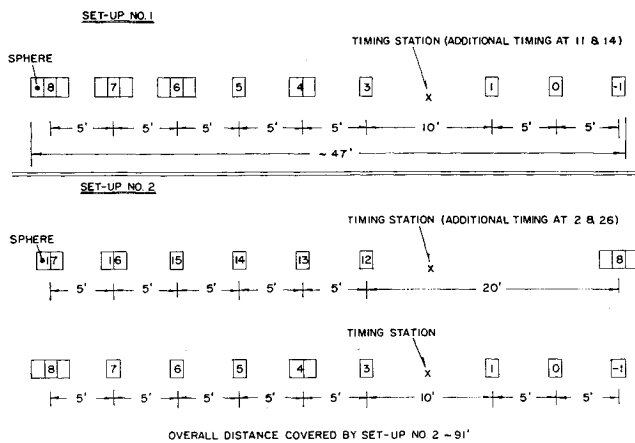
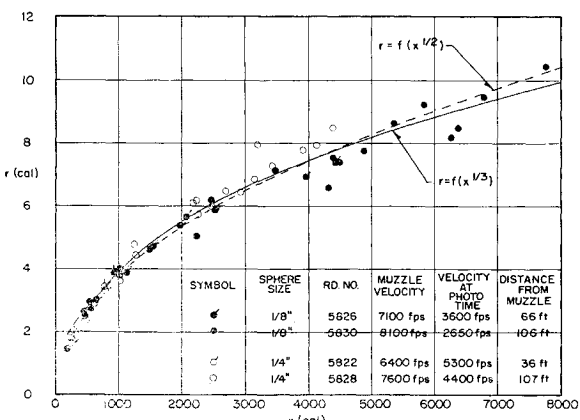
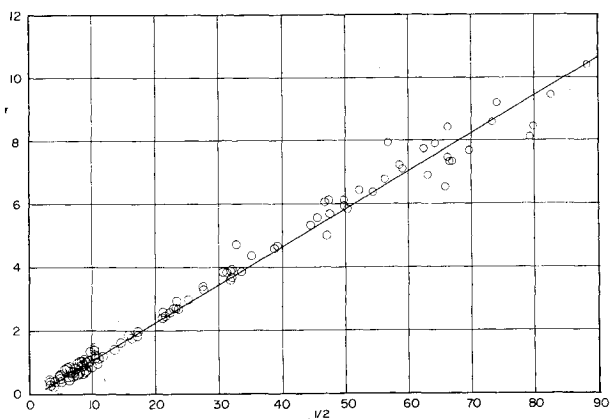
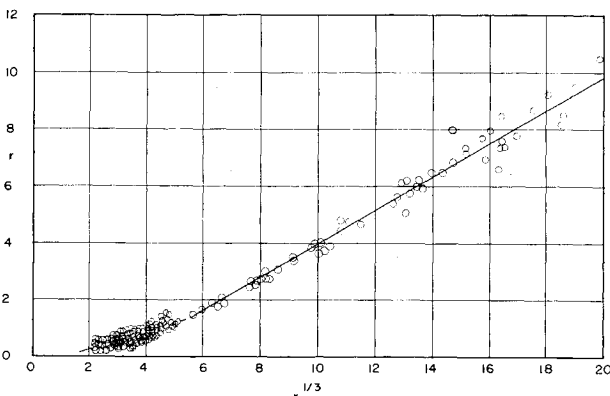


Fig. 1 Distribution of spark photography stations

Fig. 2 Wake radius vs distance from base;  $x > 200$ Fig. 3  $r$  vs  $x^{1/2}$ ;  $10 < x < 8000$ Fig. 4  $r$  vs  $x^{1/3}$ ;  $10 < x < 8000$ 

0.24.<sup>4</sup> For  $\alpha = \frac{1}{3}$ , however,  $r_0$  was significantly large ( $-2.0$ ) and would affect the log-log plot. Fig. 2 shows  $r$  plotted against  $x$ , with the two least-squares solutions drawn through the points  $r = f(x^{1/2})$  and  $r = f(x^{1/3})$ .

Figs. 3 and 4 show  $r$  plotted against  $x^{1/2}$  and  $x^{1/3}$ , respectively. In these figures, points were plotted for all values of  $x$  greater than 10 calibers. From  $x = 10$  to  $x = 200$ , all measured points were plotted; for distances greater than 200 calibers, one average per plate was plotted. It appeared that  $r$  was a linear function of  $x^{1/2}$ , and so a least-squares fit was made:

$$(r + 0.1)^2 = x/70 \quad [1]$$

For the full range of data plotted in Fig. 4, the fit definitely is not linear. It does appear, however, that the data could be approximated by a pair of lines. This may be written in the following form:

$$(r + 0.4)^3 = x/40 \quad x < 200 \quad [2a]$$

$$(r + 2.0)^3 = x/4.7 \quad x > 200 \quad [2b]$$

On the basis of the present data, there is no justification for drawing any firm conclusion on the specific dependence of  $r$  on  $x$ . The wide variation in wake width at any given distance behind the sphere was so great (Fig. 5) that one hesitates to state the nature of the dependence. This wide variation in wake width is further illustrated in Figs. 6 and 7.

Fig. 6 is a photograph of a  $\frac{1}{8}$ -in. sphere, showing approximately 100 calibers of wake. This print was made from the two plates at station 17 of round 5830. Further downstream, it becomes more difficult to see the wake in shadowgraphs and virtually impossible to obtain sufficient contrast for reproduction. In order to give a picture of the wake, the measured points from a few of the plates of round 5830 are shown plotted in Fig. 7. As mentioned previously, the measurements were made every  $\frac{1}{2}$  in. on the plate, so that the sketches show smoothed contours. This can be seen by comparing the sketch at the top of Fig. 7 with the photograph of this same section of wake, the rearward portion of Fig. 6. The sketches of Fig. 7 perhaps clarify the wide scatter of points shown in Fig. 5.

## Discussion

Slattery and Clay (7) measured the turbulent wakes of  $\frac{1}{2}$ - and  $\frac{1}{4}$ -in. aluminum spheres at atmospheric pressure and velocity of 9000 fpm and obtained the curve

$$r^2 = x/40 \quad [3]$$

This result is in direct conflict with Eq. [1]. A closer examination of their data, however, shows a definite scale effect. Eq. [3] describes the growth for the  $\frac{1}{2}$ -in. sphere, whereas the  $\frac{1}{4}$ -in. data are very well fitted by Eq. [1].

Although this  $\frac{1}{2}$ -power growth relation is a convenient way to describe the data, none of the theoretical work predicts this exponent. As can be seen from the figures for  $x > 200$ , the exponent is not very well determined. For this portion of the wake, the theories predict a  $\frac{1}{3}$ -law growth but not quite the same form as that of Eq. [2b]. Lees and Hromas, for example, predict a growth of the form

$$r^3 - bx = c \quad [4]$$

In other words, Eq. [2b] assumes a  $\frac{1}{3}$ -power growth from the point  $(0, -2.0)$ , whereas the theory predicts such a growth from  $(-c/b, 0)$ . Although  $c$  is not predicted by the theory without the introduction of a difficult analysis of the wake growth from the sphere itself,  $b$  is predicted to be  $(1.85) KC_D$ , where  $K$  is related to Townsend's invariant wake Reynolds

<sup>4</sup> When all values of  $x$  greater than 10 are used,  $r_0$  is  $-0.11$ .

Table 1 Drag coefficients estimated from the wake growth

	$10 < x < 200$	$200 < x < 8000$
Lees-Hromas	0.3	1.8
Morton	0.5	3.0

number.  $K$  is estimated from several subsonic experiments to be 0.04.

Lees and Hromas developed their theory on the assumption that the turbulent diffusivity was proportional to the product of the wake radius and its momentum defect. Morton developed a less sophisticated analysis for incompressible flow based on the assumption that the mass entrainment rate must be proportional to the momentum defect. This theory predicts  $b$  to be  $\frac{3}{8}C_D E$ , where  $E$  is the ratio of the inflow speed to the speed difference between the wake and ambient flow for an assumed top-hat profile. Morton conjectures that a good value of  $E$  is 0.116.

The data for  $x < 200$  and  $x > 200$  were fitted by Eq. [4] with the following results:

$$r^3 = (x - 35)/42 \quad 10 < x < 200 \quad [5a]$$

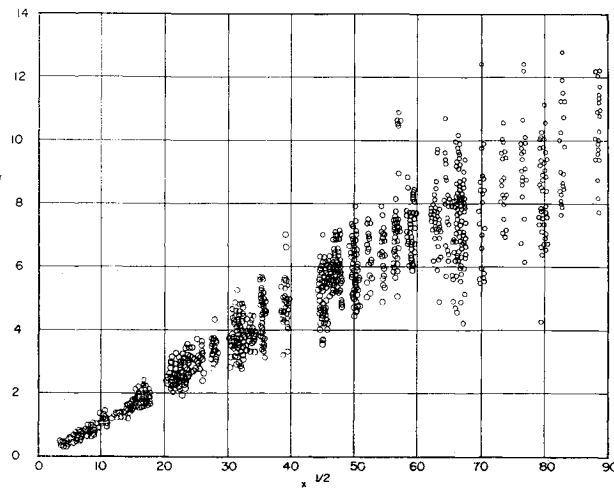
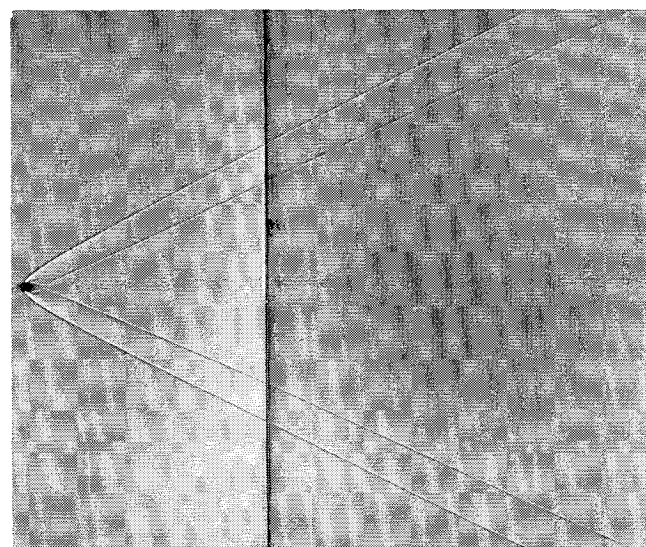
$$r^3 = (x - 610)/7.6 \quad 200 < x < 8000 \quad [5b]$$

Although [5a] and [2a] have essentially the same coefficient of  $x$ , the difference in this coefficient for  $x > 200$  is significant. This difference emphasizes the care required in proper analysis of these data. This coefficient may be used to determine drag coefficient contained in the viscous wake at two sections of the wake. Values of  $C_D$  were calculated by both the Lees-Hromas theory and the Morton theory and are given in Table 1.

This tabulation shows good agreement in order of magnitude for the total drag coefficient, which is actually a little less than unity. It is interesting to note a change in wake drag by a factor of 6 between the near and far wake. This is in reasonable agreement with the Lees-Hromas model.

One important difference exists between the theory and experiment. At atmospheric pressure, the missile velocity decays from 6800 to 2650 fps over a trajectory distance of 8000 calibers. This change in velocity is in direct conflict with the Lees-Hromas assumption of constant velocity.

In order to handle this deceleration effect, the authors will make the assumption of quasi-steady state. In other words, the velocity is assumed to be constant for sections of wake, and, for these sections, the theory with the local velocity inserted applies. Thus, the last part of the 8000-caliber long wake of Rd 5830 was generated by a sphere traveling at a constant velocity of 6800 fps. At this velocity, the missile will travel much farther than the actual decelerating missile,

Fig. 5  $r$  vs  $x^{1/2}$ ; all measured values for  $10 < x < 8000$ Fig. 6  $\frac{1}{8}$ -in. sphere at 2650 fps

and the measured wake diameter corresponds to a much larger value of  $x$ .

This effective value of  $x$  may be easily computed. For a constant drag coefficient, the missile velocity is given by the relation<sup>5</sup>

$$u = -(d)(dx/dt) = u_0 e^{C_D^* x} \quad [6]$$

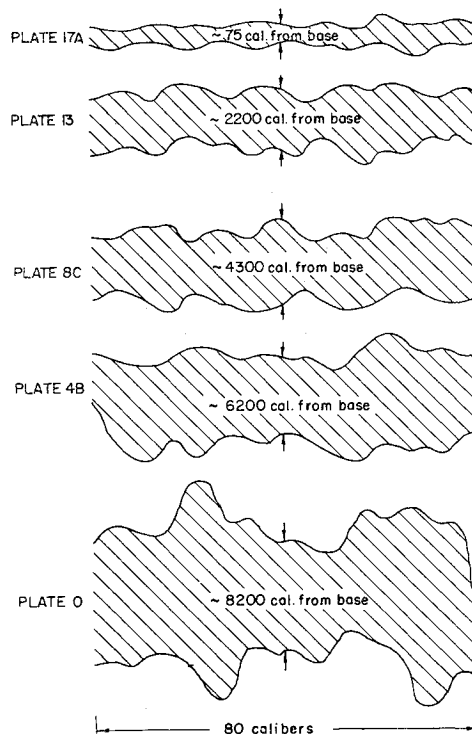
where  $u_0$  is velocity at time of shadowgraph ( $x = 0$ )

$$C_D^* = (\rho \pi d^3 / 8m) C_D$$

Eq. [6] may be integrated to yield

$$-(u_0/d)t = (1 - e^{C_D^* x})/C_D^* \quad [7]$$

The quasi-steady state assumption introduces an effective

Fig. 7 Sketches of wake from selected plates; round 5830 muzzle velocity: 8100 fps;  $\frac{1}{8}$ -in. sphere

<sup>5</sup> Since the direction of travel of the missile is opposite from the direction in which the wake coordinate  $x$  is measured, a negative sign is required in Eqs. [6] and [8].

length  $x_e$ , which a constant velocity missile would travel in time  $t$ :

$$x_e = - (u/d)t = (e^{C_D^* x} - 1)/C_D^* \quad [8]$$

Effective lengths were computed for the data of this report, and revised versions of Eqs. [2b] and [5b] obtained

$$(r + 1.2)^3 = x_e/7.9 \quad [9]$$

$$r^3 = (x_e - 415)/11.1 \quad [10]$$

Once again one sees the importance of knowing the proper form of the wake growth. From the coefficient of Eq. [10] a better value of  $C_D$  may be calculated by means of the Lees-Hromas theory. This value, 1.2, is 20% higher than the true value. Since  $K$  is certainly not any better known than 20%, this is a very encouraging verification of the Lees-Hromas theory.

### Summary

1) Experimental determination of the exponential coefficient in the growth law for a turbulent wake is very difficult, if not impossible.

2) If use is made of the theoretically predicted value of this coefficient, the existence of two distinct regions of growth

( $x < 200$ ,  $x > 200$ ) is shown by the experimental data.

3) Although the Slattery and Clay data indicate a scale effect for  $\frac{1}{4}$ -and  $\frac{1}{2}$ -in. spheres, the authors'  $\frac{1}{8}$ - and  $\frac{1}{4}$ -in. sphere data indicate at most a much weaker scale effect.

4) It is important to fit the data with the proper algebraic expression of the theoretical growth law, i.e.,  $r^3 = bx + c$ .

5) If the effect of sphere deceleration is assumed to be described by a quasi-steady state transformation, the coefficient  $b$  for the far wake is well predicted by the Lees-Hromas theory.

### References

- 1 Birkhoff, G. and Zarantonello, E. H., *Jets, Wakes and Cavities* (Academic Press, New York, 1957).
- 2 Morton, B. R., "On a momentum-mass flux diagram for turbulent jets, plumes and wakes," *J. Fluid Mech.* 10, Part 1, 101-112 (1961).
- 3 Lees, L. and Hromas, L., "Turbulent diffusion in the wake of a blunt-nosed body at hypersonic speeds," *Aeronaut. Dept. Rept. 50, Space Technology Labs. Inc.* (July 1961); also *Inst. Aerospace Sci. Paper 62-71*.
- 4 Cooper, R. D. and Lutzky, M., "Exploratory investigation of the turbulent wakes behind bluff bodies," *David W. Taylor Model Basin Rept. 963* (October 1955).
- 5 Billerbeck, W. J., Jr., "Empirical equation for the wake-spreading limits behind three-dimensional bodies," *J. Aerospace Sci.* 27, 640 (1960).
- 6 Dana, T. A. and Short, W. W., "Experimental study of hypersonic turbulent wakes," *Convair, San Diego, Calif., ZPh-103* (May 1961).
- 7 Slattery, R. E. and Clay, W. G., "Width of the turbulent trail behind a hypervelocity sphere," *Phys. Fluids* 4, 1199-1201 (1961).
- 8 Braun, W. F., "The free flight aerodynamics range," *Aberdeen Proving Ground BRL R 1048* (July 1958).

FEBRUARY 1963

AIAA JOURNAL

VOL. 1, NO. 2

## Compressible Free Shear Layer with Finite Initial Thickness

M. RICHARD DENISON\* AND ERIC BAUM†

*Electro-Optical Systems Inc., Pasadena, Calif.*

The momentum equation was uncoupled from the other conservation equations for the case of a finite initial profile in a laminar free shear layer. The equation was solved numerically, in the Crocco coordinate system, using an implicit finite difference method. Profiles of velocity and shear function were obtained as a function of streamwise distance. The initial profiles as the flow separates from the rear of the body correspond to the Blasius profile in transformed coordinates. For large distances downstream, the profiles approach the Chapman distribution, corresponding to the case of zero initial free shear layer thickness. The effect of these results on calculations of base pressure and wake angle is discussed. A method for the calculation of finite chemical kinetic effects on the profiles of temperature and chemical composition in the free shear layer with finite initial thickness is outlined.

### Nomenclature

$C$	= Chapman-Rubesin parameter, see Eq. (7)
$F$	= shear function, see Eq. (8)
$F_0$	= initial shear function
$F_w$	= initial shear function at body surface
$F^*$	= $F/F_w$
$P$	= pressure
$r_0$	= distance from axis of symmetry to body surface or dividing streamline
$S$	= transformed distance parameter, see Eq. (4)
$S_b$	= parameter $S$ evaluated for body
$S^*$	= $SCF_w^2$

Presented at the IAS Summer Meeting, Hypersonics II (Heat Transfer) Session, Los Angeles, June 19-22, 1962. Received May 11, 1962; revision received November 26, 1962. This work was sponsored by the Advanced Research Projects Agency, Washington, D.C., under ARPA Order 203-61, monitored by the Army Ordnance Missile Command, Huntsville, Ala., under Contract DA-04-495-ORD-3245.

\* Manager, Fluid Dynamics and Plasma Propulsion Department.

† Senior Scientist.

$u$	= component of velocity along dividing streamline
$u^*$	= $u/u_e$
$U$	= $u^*(3S^*)^{-1/3}$
$v$	= component of velocity perpendicular to dividing streamline
$\bar{v}$	= transformed velocity component, see Eq. (7)
$x$	= distance along dividing streamline from base of body
$y$	= distance normal to dividing streamline
$Y$	= normal distance parameter, see Eq. (3)
$\eta$	= normal distance parameter for similar solutions, see Eq. (9)
$\mu$	= viscosity
$\psi$	= stream function

### Subscripts

$D$	= dividing streamline conditions
$e$	= conditions at outer edge of free shear layer

### I. Introduction

THE length of trail behind a body, defined by observables such as electron density and radiation intensity, is de-